A damage constitutive model for sliding friction coupled to wear

Francesco d'Annibale, Angelo Luongo

Francesco D'Annibale · Angelo Luongo

A damage constitutive model for sliding friction coupled to wear

Abstract Several new constitutive models are formulated for the planar interface of a soft body sliding on a rigid soil, describing stick-slip phenomena due to friction, and wear due to abrasion. Attention is focused on damage at the interface, by neglecting any interaction with damage of body and any propagation of damage inside the body. Models are formulated in the general framework of the Thermodynamics of the irreversible processes and account for suitable defined internal variables of phenomenological type, namely gap, isotropic friction hardening and wear. The main feature of the new presented models is that the formulation of the wear process at the interface is obtained in the contest of Damage Mechanics, and it is based on the formal analogy between abrasion of a soft body and ductile damage of an elastic-plastic material. By following this approach, a scalar wear field, an effective stress and appropriate state and dissipation potentials are defined, able to describe a tangential isotropic wear process due to stick-slip and to hardening mechanism. Both cases of linear and nonlinear friction hardening are formulated; moreover, wearable and no-wearable bodies are considered. Numerical results relevant to one-dimensional problems are illustrated for monotonic, forward-backward and cyclic displacement time-histories, showing evolution for stress, gap and wear. Results furnished by different models are compared and discussed.

Keywords Damage · Friction · Quasi-static contact · Wear

1 Introduction

When a body is loaded by monotonous or cyclic loads, it undergoes a progressive stiffness reduction, caused by a time-decay of its mechanical properties. The description of such degradation phenomenon, which has been object of many scientific studies, is a task of a branch of Solid Mechanics, known as Damage Mechanics [1–3]. According to this approach, the material behavior is described in the framework of the Thermodynamics of the irreversible processes, by making use, in addition to the usual observable variables, of internal (not observable) variables. The set of all the (observable and not observable) variables is postulated to univocally describe the "state" of the material, thus avoiding to account for its memory.

F. D'Annibale · A. Luongo (✉)
Dipartimento di Ingegneria Civile, Edile-Architettura e Ambientale, University of L'Aquila, 67100 L'Aquila, Italy
E-mail: angelo.luongo@univaq.it
Tel.: +39-0862-434521
Fax: +39-0862-434548

F. D'Annibale
E-mail: francesco.dannibale@univaq.it
Tel.: +39-0862-434523
Fax: +39-0862-434548

When a body is made by several layers, or, equivalently, a homogeneous body slides on the soil, a new form of damage appear, the *wear*, initially localized at the interface(s), and possibly propagating inside the body. Although other forms of wear exist (namely by adherence, corrosion and superficial fatigue, see [4–6]), wear produced by abrasion is of interest here, as a consequence of stick-slip phenomena [7–9]. Wear has been extensively studied in Tribology [10] in a wider context of surface interactions. It consists in the slow and continuous removal of a generally small amount of material from a solid surface, and it occurs when a hard material slides on a softer material, leading to separation of fragments of the original asperities of this latter [11,12]. Such particles, when interposed between the two bodies, can facilitate or impede the sliding, according to their small or large dimensions, respectively. Therefore, artificial interposition of small fragments is also used for lubrication purposes [13–15].

The studies cited, however, have often been conducted on a phenomenological ground, and have led to empirical laws, aimed to establish, for example, the dimension of fragments, the useful life of a machinery, and so on. In [16], for example, the influence of repeated uni-directional sliding for the prediction of wear in sliding metallic friction is analyzed by considering a wedge which slides over of a surface of the same length. In [17], another point of view is enveloped: the characteristic deformation of the contact layer is explained in terms of the wave model of asperity deformation and surface damage is analyzed by considering the strain cycle undergone by material as it flows through the wave.

A way to give a mathematical description of the contact phenomena like friction and wear in quasi-static regime, object of many scientific studies (e.g., [18–21]), is to introduce the concept of "interface": a plane (or curved) layer endowed (or not) with material properties and with vanishing (or not) volume. The presence of interfaces plays a fundamental role in several physical phenomena appearing in different frameworks, such as diffusion and interfacial exchange in a porous media (see, for instance, [22]) or electrical conduction in biological tissues (see [23–25]), or fiber reinforced materials (see [26]). Mathematical modeling of interface between contact surfaces and of its constitutive behavior can be interpreted as an extensions of the phenomenological ground and of the experimental information to a better understanding and simulating friction, damage and crack phenomena.

Thermodynamics and Damage Mechanics afford the possibility of a theoretical description of the thermomechanical phenomena occurring in rubbing and wearing systems; so, in the present paper, a thermodynamical damage constitutive model for a Cauchy's interface is built, able to take into account different (coupled) interfacial phenomena, like adhesion, friction, hardening effects and wear.

The spirit of the present work is similar to the one animating the papers [27–30], in which a thermodynamical model of contacting solids is built and a set of dependent variables describing the material properties of the bodies, the interfacial layer of wear products and the contact are derived; in [27–29], the contact is described by introducing the definition of a two-dimensional micropolar interfacial layer and its definition is enriched with a description of the constitutive equations for friction, wear and frictional heat. Moreover, in [30], the theory of metal fracture is applied to wear and the non-monotonic character of damage accumulation has been taken into account.

Other relevant examples of mathematical modeling of interface between solids in contact can be found in [31–35], where the considered interfaces are endowed with material properties like surface mass density, linear momentum, energy or entropy. In such more sophisticated models, extra surface kinematical descriptors need to be considered, and correspondingly, new balance equations need to be postulated, in order to determine their evolution equations. A different approach, based instead on the application of a Hamilton–Rayleigh dissipation principle may be also viable, by generalizing the results presented in [36].

However, although the mechanisms of wear consists in a kind of damage for the interface(s), modeling of wear phenomena does not seem to have received sufficient attention in the contest of Damage Mechanics in the meaning of [2,3]. Few exceptions are represented by the papers [37,38]. In [37], a generalized standard interface constitutive model for wearing contact is derived; then, a two degrees of freedom system with a one-point contact is considered, with thermal effects neglected, and the existence and uniqueness of the solution is discussed. In [38] a beam with a tip in wearing contact with a moving rigid surface is studied; propagation and distribution of damage along the beam is analyzed by using a nonlocal damage model.

Due to the scientific relevance of the topic and its importance in many engineering applications, it would be worth to formulate the problem of wear in the context of Damage Mechanics. This paper is an initial attempt toward this end. Here, attention is focused on damage at the interface, by neglecting any interaction with damage of body and any propagation of damage inside the body.

Several damage models are formulated, by exploiting the formal analogies, (a) between friction and plasticity and (b) between abrasion of a soft body (quasi-statically) sliding on hard soil and ductile damage of an

elastic-plastic material. Models describe the mechanisms of superficial interaction through an ideal contact interface, defined as a two-dimensional body of evanescent thickness, interposed between the body and the soil and bonded to them, endowed with material properties and capable of shear strains only.

Interface constitutive laws are defined in the framework of the Thermodynamics of irreversible processes and of the theory of internal variables. A scalar surface field w, as a measure of the "wearing capability" at interface, is introduced and it is defined as an internal variable which can only increase with respect to time, its growth being related to an increasing "smoothness" of the interface and, consequently, to a decrease of its abrading capabilities. Although a more refined approach would require the introduction of a tensor surface field, in the present paper, a scalar one is considered. This limitation is essentially equivalent to assume a tangential isotropic wear process and represents a first generalization of the models proposed in [39–41]. Under the hypothesis of additive decomposition (elastic and inelastic) of interface strains and of validity of the equivalent strain principle, the Helmholtz free energy is chosen as a state potential and it is assumed to be additive in its elastic and inelastic parts, respectively. Thermal dissipative effects are neglected, thus referring to an ideal isothermal process, and the dissipation potential is assumed to be additive in its stick-slip and wear parts, respectively; for these reasons, flow laws, whose time-evolution is able to describe stick-slip and wear phenomena at the interface, are associated for stick-slip variables and not associated for wear.

It should be remarked the fact that the models, presented in this paper, have some resemblances with plasticity and softening in damage mechanics and that these analogies are exploited for driving a formal presentation. To the authors' knowledge, the introduction of such an internal wear parameter, coupled with plastic interfacial phenomena, is an original feature of the interface constitutive models.

The paper is organized as follows. In Sect. 2, some introductory concepts are illustrated and analogies with plasticity of damaged solids are stressed. In Sect. 3, the constitutive law for the interface is formulated in the framework of a thermodynamic approach, once a suitable choice for the internal variables has been made. For different state and dissipation potentials, several models are obtained. They are discussed in Sect. 4 for purely friction no-wearable bodies, and in Sect. 5 for wearable bodies. Results of several numerical integrations are commented in Sect. 6 for one-dimensional problems and different displacement time-histories. Finally, some conclusions are drawn in Sect. 7.

2 Basic models and analogies

Some basic ideas concerning friction and wear are introduced here. Moreover, formal analogies with other models of Solid Mechanics are shortly discussed.

A rigid block is considered, in quasi-static contact with soil, loaded by a normal force $P = \text{const}$ and a tangential force $F(t)$, depending on time (Fig. 1). Due to the contact between the solids, a tangential friction force $T(t)$ arises. Two alternatives can occur, namely (a) the force F is not sufficient to trigger any motions (*stick-phase*, Fig. 1a), or, (b) it produces a tangential motion (*slip-phase*, Fig. 1b). In the classical theory of friction, T is expressed in terms of macroscopically observed quantities. It is postulated (Coulomb law) that: (a) in the stick-phase, the force T is equal and opposite to the force F; (b) in the slip-phase, the force T is opposite to the direction of the motion, constant in time and its intensity is proportional to P, that is, $T_{\max} = \mu P$ with μ the *friction coefficient*; moreover, it is independent both of the apparent contact area and of the sliding velocity. Therefore, in order to the block moves of uniform motion, F must be kept constant and equal to $T_{\max}$.

When, however, experimental shear tests are performed on a block of ductile material, loaded by a normal force $P = P_i$ and by a tangential force F, results as those sketched in Fig. 2 are obtained [19]. The plot shows the modulus $|T|$ of the friction force versus the tangential displacement u of the body, when three different

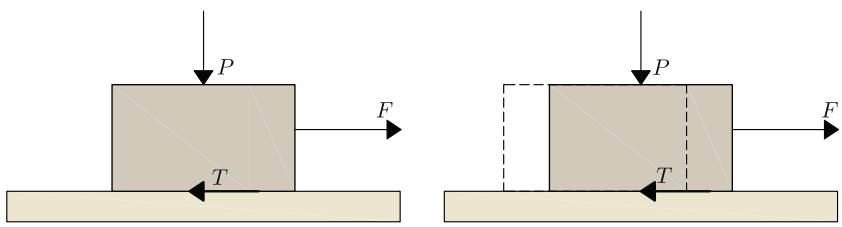

Fig. 1 Rigid body on a planar soil: P normal force, F tangential force, T friction force: **a** stick-phase, **b** slip-phase

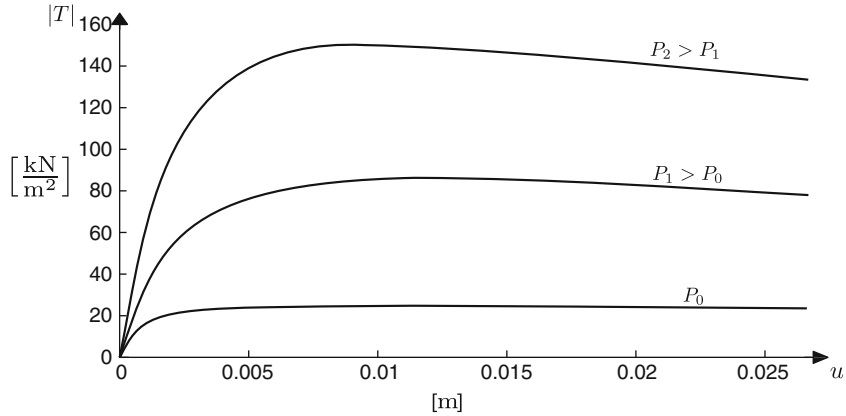

Fig. 2 Experimental friction force modulus $|T|$ versus displacement u for the block in Fig. 1, reported in [19]: $P_0 = 25\ \frac{\text{kN}}{\text{m}^2}$, $P_1 = 100\ \frac{\text{kN}}{\text{m}^2}$, $P_2 = 200\ \frac{\text{kN}}{\text{m}^2}$

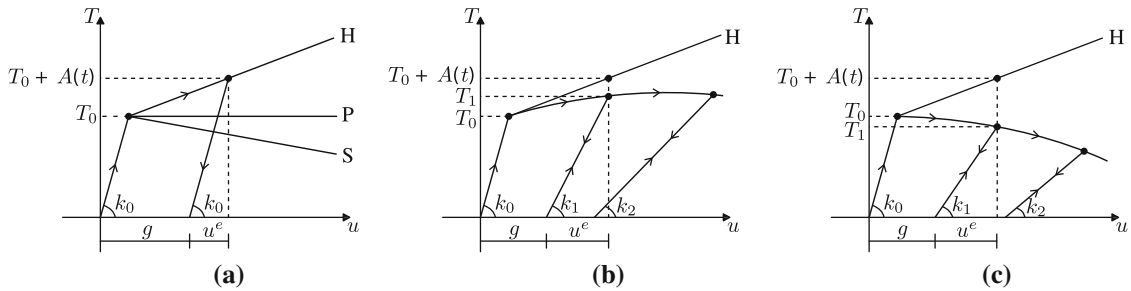

Fig. 3 Constitutive models for friction and wear: **a** no-wear model, of perfect (P), hardening (H) or softening (S) type; **b** weak wear model; **c** strong wear model

normal forces, namely $P_0 = 25\,\text{kN/m}^2$, $P_1 = 100\,\text{kN/m}^2$ and $P_2 = 200\,\text{kN/m}^2$, are applied. It is seen that the response is initially linear, with (positive) slope increasing with P. Successively, the slope progressively decreases and monotonically tends to zero, when the normal force is low ($P = P_0$), or it becomes first negative and then comes back to zero (for very large displacements) when the normal force is medium/high ($P = P_1$, $P = P_2$). Therefore, for quasi-static behavior, $u(t)$ must be slowly varied in time and, moreover, $F(t) = T(u(t))\ \forall t$, that is, the experiment must be displacement-controlled.

The experimental results of Fig. 2 suggest the following theoretical interpretation, based on a micro-modeling of the contact. Both the block and the soil are not smooth, but small asperities exist, mutually framed and kept in contact by the normal force. When a small tangential force is applied, the asperities deform themselves elastically, mainly for shear, producing a small tangential displacement of the body, but still remaining trapped (stick-phase). In this phase, the larger the normal force, the larger the stiffness of the body, due to (a) the shortening of asperities, caused by compression (elastic stiffness) and (b) a small normal displacement of the body, requiring a negative work of the force P to be done (geometric stiffness). In order a larger displacement occurs (slip-phase), the asperities of the body must overtake those of soil, this requiring a tangential force threshold $T_{\text{lim}} = T_0$ to be reached, where T_0 denotes a property of the virgin material. Some authors also conjecture the existence of molecular links among asperities, produced by adhesion, which must be broken, before the motion can take place [13,14]. After that, the motion would continue indefinitely at the same value of force, if the state of the asperities did not evolve with the motion itself (Fig. 3a, perfect curve P). Analogy with the elastic-perfect plasticity is evident. This is what happens in the test when the normal force is low; however, this is not the case when the force is higher, as explained soon.

First, the existence of wear is excluded, and friction alone is considered (Fig. 3a, no-wear model NW). During the motion, the tips of the asperities are loaded by tangential and normal stresses, eventually leading the material to enter the plastic regime. Caused by the re-iterated up and over the soil asperities, each asperity of the block undergoes load-unload cycles, which call for additional plastic work to be spent by the external force, with respect to the stick-phase. If the material possesses a hardening (softening) behavior, each cycle entails an increasing (decreasing) amount of energy to be spent to sustain the motion, resulting in a hardening

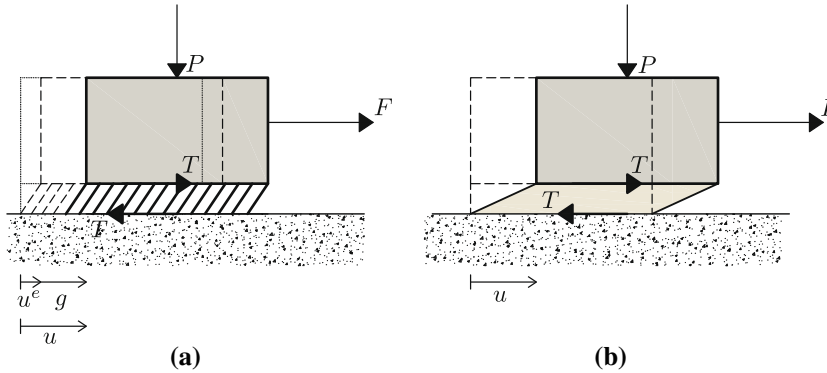

Fig. 4 Rigid body sliding on a rigid soil: **a** elastic asperities, g gap, u^e elastic displacement, u total displacement; **b** elastic-plastic interface

(softening) macroscopic behavior, as illustrated in Fig. 3a (curves H and S). Hardening (softening) also entails that, after an unload-reload cycle, the threshold value of the friction modifies as $T_{\lim}(t) = T_0 + A(t)$, where $A(t)$ denotes the *isotropic hardening/softening* of friction at time t ($A > 0$ hardening, $A < 0$ softening), which is a function of the displacement history. Analogy with the plasticity of solids with isotropic hardening is self-evident. This phenomenon explains the (initially) hardening behavior of the experimental results in Fig. 2, at medium-high normal forces.

To explain the subsequent softening, wear must be accounted for. Due to an excess of plastic deformation, tips of the asperities detach themselves from the body, and small material particles fall down on the soil. This phenomenon entails a *damage*, in the sense that several asperities of the body are no more in contact with the asperities of the soil, so that the contact area decreases. Wear therefore can be defined as the ratio $w := S_d/S$ between the damaged contact area and the original undamaged contact area. Accordingly, $w = 0$ denotes an undamaged surface, and $w = 1$ an entirely damaged surface (limit case, unreachable). Damage reduces the elastic-geometrical stiffness, since it reduces the number of asperities; moreover, it also decreases the resistance to the motion in the slip-phase because of the lubrication effect played by the interposed particles. Therefore, wear introduces softening in the mechanical behavior, in accordance with experimental tests. An idealized load-history, for a hardenable material, is sketched in Fig. 3b, c, where few unload-reload paths are considered, showing progressive reduction of the slope of the paths, both in stick- and slip-phases. In particular, a weak wear (WW) and a strong wear (SW) effects are considered in Fig. 3a, b, respectively, causing the threshold of the slip-phase to move up or down the limit value T_0 of the corresponding no-wear hardening model.

To evaluate the reduction of the stiffness and of the threshold caused by wear, it is worth noticing analogy with damage mechanics of material. An *effective tangential force* $\tilde{T} := T/(1-w)$ is defined, as the fictitious force acting on the undamaged contact area, producing the same strain of the true force T acting on the damaged contact area. By applying the so-called *equivalent strain principle* [2], all the relations holding for the undamaged body, still hold for the damaged body, provided T is replaced by $\tilde{T}$. Therefore, both the elastic stiffness k_0 and the threshold $T_0 + A(t)$ are reduced by the factor $(1-w)$, thus becoming $k_1 := k_0(1-w)$ and $T_1 := (T_0 + A(t))(1-w)$ (see Fig. 3b, c).

Previous consideration can be formalized in a mathematical form, by exploiting analogies with plasticity and damage. First, however, the concept of "interface" must be introduced, in order to avoid to deal with discontinuities in the displacement field, when relative motions between block and soil occur. To this end, one can think to substitute the"real" discrete asperities (Fig. 4a), with an "ideal" vanishingly small layer of deformable material, capable of shear strains only and bonded to the two bodies which is interposed (Fig. 4b). Second, it is observed that the displacement u of the body consists in an elastic part u^e, in which the tips of the (deformed) asperities are still in contact with the soil (stick-phase), and in an inelastic part g, which describes the sliding of the tips (slip-phase), usually referred to as the *gap*; therefore, the decomposition $u = u^e + g$ holds.

The constitutive law for the interface, in incremental form, consists of a state law (elastic):

$$\dot{T} = k(\dot{u} - \dot{g}) \tag{1}$$

and a flowlaw:

$$\dot{g} = \begin{cases} 0 & \text{if } |T| < T_{\text{lim}} \\ 0 & \text{if } |T| = T_{\text{lim}} \quad \text{and} \quad \dot{T} < 0 \\ \dot{\lambda}\,\text{sign[T]} & \text{if } |T| = T_{\text{lim}} \quad \text{and} \quad \dot{T} = 0 \end{cases} \tag{2}$$

where a dot denotes time-differentiation and $\dot{\lambda} > 0$ is a scalar quantity. In Eqs. (1) and (2), the stiffness, k, and the threshold value of the tension, T_{lim}, depend on the model adopted for the interface. (a) For non-hardening and no-wear interface, they coincide with those of the virgin material, namely $k = k_0$ and $T_{\text{lim}} = T_0$, in analogy with perfect plasticity. (b) For the hardening/softening and no-wear interface, it is still $k = k_0$, but $T_{\text{lim}} = T_0 + A\,(t)$, where $A(t)$ is a function of the *total gap*, namely $\alpha(t) := \int_0^t |\dot{g}(t)|\,\mathrm{d}t$, of the motion history, which represents the *isotropic friction hardening*, and it is analogous to the isotropic hardening variable of plasticity theory; Eqs. (1) and (2) must be sided by a flow equation for $\alpha(t)$ and by a state equation linking the dual variables $A(t)$ and $\alpha(t)$. (c) For the hardening/softening and wearable interface, it is $k = k_0(1 - w(t))$ and $T_{\text{lim}} = (T_0 + A(t))\,(1 - w(t))$, where the hardening $A(t)$ depends on the *effective total gap*, namely $\alpha(t) := \int_0^t |\dot{g}(t)|\,/(1 - w)\mathrm{d}t$ and, moreover, on $w(t)$ in analogy with damage mechanics of elastic-plastic solids. Therefore, formulation calls for a new flow law for $w(t)$ and for a new state law for its dual variable $W(t)$, having the physical meaning of *energy density release rate* [2,3].

In conclusion, when the motion takes place along a rectilinear trajectory, the constitutive laws for interface assume the (incremental) form:

$$\begin{aligned} \dot{\mathbf{X}} &= \mathbf{f}(\dot{u}, \dot{\mathbf{x}}) \\ \dot{\mathbf{x}} &= \mathbf{h}(\mathbf{x}, \mathbf{X}, \dot{\mathbf{X}}) \end{aligned} \tag{3}$$

where $\mathbf{f}$ and $\mathbf{h}$ are constitutive functions and, in the general case, $\mathbf{X} := (T, A, W)^T$, $\mathbf{x} := (g, \alpha, w)^T$ are the vectors of dual and internal variables, respectively.

3 An internal variable constitutive model for interface

Let us consider a deformable body $\mathcal{B}_d$ in contact with a planar rigid surface $\mathcal{S}_r$ (soil) lying in the (x, y)-plane (Fig. 5a). A thin deformable cylindrical interface $\mathcal{B}_c$ is interposed between the body and the surface, of thickness b, and bases S_c^+ and S_c^-, of unit normal vectors $\mathbf{n}_c^+$ e $\mathbf{n}_c^-$, respectively, parallel to the z-axis (Fig. 5b). Surface S_c^- is bonded to the soil while surface S_c^+ is bonded to the body, and it experiences a tangential displacement field $\mathbf{u} = \mathbf{u}(x, y)$. The following assumptions, based on the small thickness of $\mathcal{B}_c$, are introduced: (a) the interface is capable of shear strains only; (b) the shear strains and shear stresses are constant along its thickness (Fig. 5c), that is, $\boldsymbol{\gamma} = \boldsymbol{\gamma}(x, y)$, $\boldsymbol{\tau} = \boldsymbol{\tau}(x, y)$. These vectors, in the (x, y)-basis, admit the following

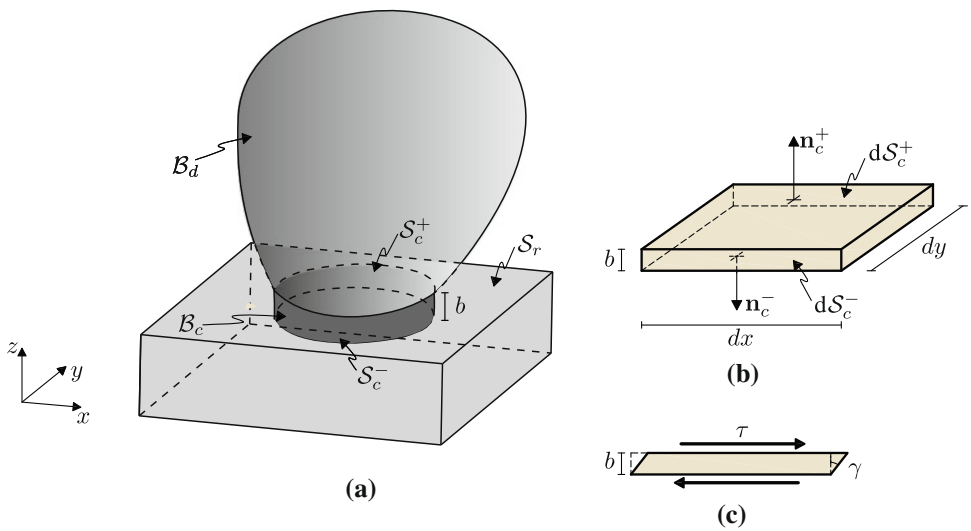

Fig. 5 Contact scheme: **a** deformable body sliding on a fixed rigid surface; **b, c** contact interface

scalar representation: $\mathbf{u} = (u_x, u_y)^T$,$\boldsymbol{\gamma} = (\gamma_{zx}, \gamma_{zy})^T$, $\boldsymbol{\tau} = (\tau_{zx}, \tau_{zy})^T$. All these assumptions are similar to those formulated in [42].

Additional hypotheses are introduced for the interface body: (c) the absolute temperature ϑ is constant along z, that is, $\theta = \theta(x, y)$, but it differs from the temperatures at the bases S_c^+ and S_c^-, equal to $\theta^+ = \theta^+(x, y)$ and $\theta^- = \theta^-(x, y)$, respectively; (d) the heat flow across the mantle of the cylinder is negligible.

3.1 Thermodynamics and internal variable formulation

Aimed to formulate a constitutive model for the interface, the Internal Variables Theory for Standard Generalized Material is applied [43–49]. First, the two principles of Thermodynamics are written in local form as follows:

$$\begin{aligned} \dot{u} &= \boldsymbol{\tau}^T \dot{\mathbf{u}} - h^+ - h^- \\ \dot{s} &+ \frac{h^+}{\vartheta^+} + \frac{h^-}{\vartheta^-} \geqslant 0 \end{aligned} \tag{4}$$

as a consequence of the previous hypotheses. Here, u and s are the surface densities of the internal energy and entropy, respectively; $h^+ := \mathbf{h}^+ \cdot \mathbf{n}_c^+$ and $h^- := \mathbf{h}^- \cdot \mathbf{n}_c^-$ are the surface densities of thermal flows $\mathbf{h}^+, \mathbf{h}^-$, leaving the surfaces S_c^+ and S_c^-, respectively. By introducing the Helmholtz function, $\psi := u - \vartheta s$, the Thermodynamic principles (4) are restated in the equivalent forms:

$$\dot{\psi} = \boldsymbol{\tau}^T \dot{\mathbf{u}} - (\vartheta s)^{\cdot} - h^+ - h^- \tag{5}$$

$$\dot{\psi} - \boldsymbol{\tau}^T \dot{\mathbf{u}} + s\dot{\vartheta} + \frac{h^+}{\vartheta^+}\Delta\vartheta^+ + \frac{h^-}{\vartheta^-}\Delta\vartheta^- \leqslant 0 \tag{6}$$

in which $\Delta\vartheta^+ := \vartheta^+ - \vartheta$, $\Delta\vartheta^- := \vartheta^- - \vartheta$ are the thermal jumps at S_c^+ and S_c^-.

As a second step, a *state potential* and a *dissipation potential* are introduced. The former, which is function of the (observable and internal) state variables, defines the state laws between thermodynamically associated variables; the latter, which is function of the associated variables (thermodynamic forces), defines the evolution of the internal variables and therefore the dissipation flow. The observable variables considered here are as follows: (i) the displacement $\mathbf{u}(x, y)$ at the contact and (ii) the absolute interface temperature $\vartheta(x, y)$. The internal variables considered are as follows: (i) the *gap* $\mathbf{g}(x, y)$, resulting from the decomposition $\mathbf{u}(x, y) = \mathbf{g}(x, y) + \mathbf{u}^e(x, y)$, where $\mathbf{u}^e(x, y)$ is the stick part of displacement, (ii) the *isotropic hardening* variable $\alpha(x, y)$; (iii) the *wear* $w(x, y)$.

3.2 State potential and dissipated energy

The Helmholtz free energy is chosen as a state potential and, under the hypothesis of additive dependence of free energy from $\mathbf{u}$ and $\mathbf{g}$, it reads:

$$\psi = \psi(\mathbf{u} - \mathbf{g}, \vartheta, \alpha, w) \tag{7}$$

By differentiating Eq. (7) with respect to its arguments, substituting in Eq. (6) and observing that $\partial\psi/\partial\mathbf{g} \equiv -\partial\psi/\partial\mathbf{u}$, Eq. (6) reads:

$$\left(\frac{\partial\psi}{\partial\mathbf{u}} - \boldsymbol{\tau}\right)^T \dot{\mathbf{u}} - \left(\frac{\partial\psi}{\partial\mathbf{u}}\right)^T \dot{\mathbf{g}} + \left(\frac{\partial\psi}{\partial\vartheta} + s\right)\dot{\vartheta} + \frac{\partial\psi}{\partial\alpha}\dot{\alpha} + \frac{\partial\psi}{\partial w}\dot{w} + \frac{h^+}{\vartheta^+}\Delta\vartheta^+ + \frac{h^-}{\vartheta^-}\Delta\vartheta^- \leqslant 0 \tag{8}$$

Moreover, by assuming that the thermodynamic state in the reversible processes, in which Eq. (8) must be taken with the equals sign $\forall\dot{\mathbf{u}}$, $\forall\dot{\vartheta}$, respectively, depends only from observable variables, two state laws are obtained:

$$\begin{aligned} \boldsymbol{\tau} &= \frac{\partial\psi}{\partial\mathbf{u}} \\ s &= -\frac{\partial\psi}{\partial\vartheta} \end{aligned} \tag{9}$$

together with the *dissipation inequality*:

$$\boldsymbol{\tau}^T \dot{\mathbf{g}} - A\dot{\alpha} + W\dot{w} - \frac{h^+}{\vartheta^+}\Delta\vartheta^+ - \frac{h^-}{\vartheta^-}\Delta\vartheta^- \geqslant 0 \tag{10}$$

where the following associated variables have been defined:

$$\begin{aligned} A &:= \frac{\partial \psi}{\partial \alpha} \\ W &:= -\frac{\partial \psi}{\partial w} \end{aligned} \tag{11}$$

Equation (10) expresses the fact that energy can be dissipated in three forms: (i) dissipation due to slip, $D_s := \boldsymbol{\tau}^T \dot{\mathbf{g}} - A\dot{\alpha}$; (ii) dissipation due to wear, $D_w := W\dot{w}$; (iii) thermal dissipation $D_{\Delta\vartheta} := -h^+\Delta\vartheta^+/\vartheta^+ - h^-\Delta\vartheta^-/\vartheta^-$. As usually accepted, it is assumed here that thermal dissipation is uncoupled from the other two, so that Eq. (10) splits into two inequalities, namely $D_s + D_w \geqslant 0$, $D_{\Delta\vartheta} \geqslant 0$. In the following, thermal effects will be neglected, thus referring to ideal isothermal processes; moreover, the Helmholtz free energy will be chosen in the additive form:

$$\psi\left(\mathbf{u} - \mathbf{g}, \alpha, w\right) = \psi^e\left(\mathbf{u} - \mathbf{g}, w\right) + \psi^{in}\left(\alpha, w\right) \tag{12}$$

where $\psi^e\left(\mathbf{u} - \mathbf{g}, w\right)$ and $\psi^{in}\left(\alpha, w\right)$ are the elastic and inelastic parts of the energy, respectively. It should be noticed, that, in order to take into account lubrication effects and differently from standard ductile damage models, wear also enters the inelastic part of the energy.

It should be remarked that, in the present treatment, the constrained kinematical descriptors, relative to compressibility of the interface, and related Lagrange multipliers are not included. A more detailed description of abrasion phenomena would require the introduction of these extra descriptors (as done, e.g., in [50]).

3.3 Dissipation potential

The dissipation potential is a scalar function of the thermodynamic forces $\boldsymbol{\tau}$, A and W. However, to account for damage effects, and according to the strain equivalence principle, the stress $\boldsymbol{\tau}$ is substituted by the effective stress $\tilde{\boldsymbol{\tau}} := \boldsymbol{\tau}/(1-w)$ so that, the dissipation potential reads:

$$\varphi = \varphi\left(\tilde{\boldsymbol{\tau}}, A, W\right) \tag{13}$$

This potential needs to be sided by a (control) *slip-function* $F = F\left(\tilde{\boldsymbol{\tau}}, A\right)$, able to establish, at each time, the state of the interface, namely adherence or slip-wear. From a geometrical point of view, the slip-functions are a family of closed curves, lying on the (τ_{zx}, τ_{zy})-plane, parameterized by the thermodynamic force A and by the wear w. Each curve is a boundary of a domain such that: (a) internal points characterize adherence-states, (b) boundary points denote slip-states, (c) external points cannot be reached, unless the domain is up-dated.

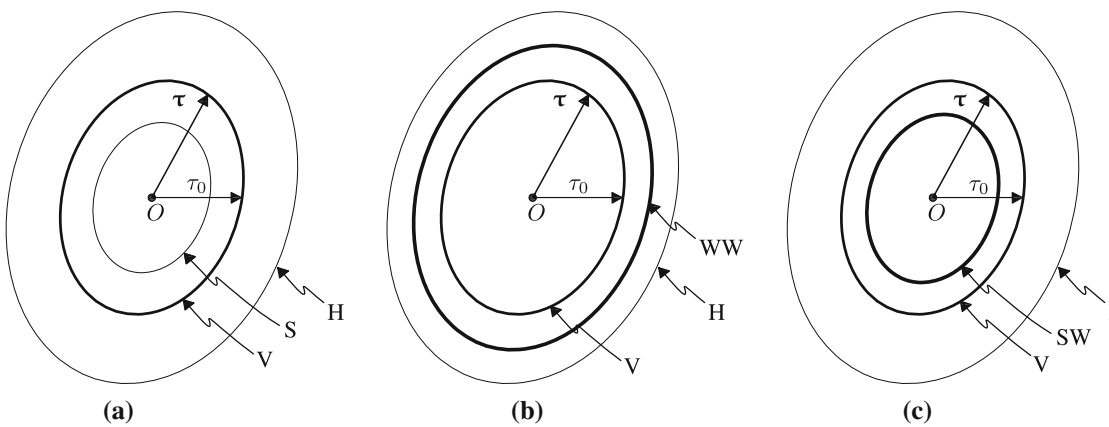

Fig. 6 Evolution of the slip-function in the (τ_{zx}, τ_{zy})-plane (V virgin state, H hardening state, S softening state): **a** no-wear (NW) model; **b** weak-wear (WW) model; **c** strong-wear (SW) model

Evolution of the domain depends on A and w, as depicted in Fig. 6 for three typical cases: no-wear (NW, Fig. 6a), for which the virgin state (V) evolves to a hardening (H) or softening (S) state; weak wear (WW, Fig. 6b) and strong wear (SW, Fig. 6c), for which a weak/strong softening effect is introduced by damage. The figure generalizes to a bi-dimensional problem the discussion made in Sect. 2 (Fig. 3).

The flow laws for the internal variables then follow from the control function and from the dissipation potential (13); by adopting the normality rule to the dissipation potential, they read:

$$
\begin{aligned}
\dot{\mathbf{g}} &= \begin{cases} \mathbf{0} & \text{if } F\left(\tilde{\boldsymbol{\tau}}, A\right) < 0 \\ \mathbf{0} & \text{if } F\left(\tilde{\boldsymbol{\tau}}, A\right) = 0 \quad \text{and} \quad \dot{F}\left(\tilde{\boldsymbol{\tau}}, A\right) < 0 \\ \dot{\lambda}\left(\partial\varphi/\partial\boldsymbol{\tau}\right) & \text{if } F\left(\tilde{\boldsymbol{\tau}}, A\right) = 0 \quad \text{and} \quad \dot{F}\left(\tilde{\boldsymbol{\tau}}, A\right) = 0 \end{cases} \\
\dot{\alpha} &= \begin{cases} 0 & \text{if } F\left(\tilde{\boldsymbol{\tau}}, A\right) < 0 \\ 0 & \text{if } F\left(\tilde{\boldsymbol{\tau}}, A\right) = 0 \quad \text{and} \quad \dot{F}\left(\tilde{\boldsymbol{\tau}}, A\right) < 0 \\ -\dot{\lambda}\left(\partial\varphi/\partial A\right) & \text{if } F\left(\tilde{\boldsymbol{\tau}}, A\right) = 0 \quad \text{and} \quad \dot{F}\left(\tilde{\boldsymbol{\tau}}, A\right) = 0 \end{cases} \\
\dot{w} &= \begin{cases} 0 & \text{if } F\left(\tilde{\boldsymbol{\tau}}, A\right) < 0 \\ 0 & \text{if } F\left(\tilde{\boldsymbol{\tau}}, A\right) = 0 \quad \text{and} \quad \dot{F}\left(\tilde{\boldsymbol{\tau}}, A\right) < 0 \\ \dot{\lambda}\left(\partial\varphi/\partial W\right) & \text{if } F\left(\tilde{\boldsymbol{\tau}}, A\right) = 0 \quad \text{and} \quad \dot{F}\left(\tilde{\boldsymbol{\tau}}, A\right) = 0 \end{cases}
\end{aligned}
\tag{14}
$$

in which $\dot{\lambda}$ is a scalar positive parameter.

Once the flow laws and the dissipation potential are defined, Eq. (10) can be re-written as follows:

$$
\dot{\lambda}(\nabla\varphi)^T\left(\boldsymbol{\tau}, A, W\right) \geqslant 0 \tag{15}
$$

which clarifies the fact that the dissipation inequality, Eq. (10), is satisfied if $\dot{\lambda} \geqslant 0$ and φ is a convex function of the associated variables.

In the following, consistently with the hypotheses introduced on dissipation [Eq. (10)], the dissipation potential will be splitted as:

$$
\varphi\left(\tilde{\boldsymbol{\tau}}, A, W\right) = F\left(\tilde{\boldsymbol{\tau}}, A\right) + \varphi_W\left(W\right) \tag{16}
$$

in which F is the slip-function and φ_W is the part of the potential which is responsible for the wear evolution. From this choice, it follows that Eq. ($14_{\mathrm{a,b}}$) are associated laws (since $\partial\varphi/\partial\boldsymbol{\tau} \equiv \partial F/\partial\boldsymbol{\tau}$ and $\partial\varphi/\partial A \equiv \partial F/\partial A$), while Eq. ($14_{\mathrm{c}}$) is a non-associated law (since $\partial\varphi/\partial W \neq \partial F/\partial W$).

Concerning the evolution of wear, and in order to reproduce experimental results, it is convenient to limit the value of this variable at a critical value $w_c < 1$. This upper bound represents the value of wear at which the interface must be considered totally broken.

The parameter $\dot{\lambda}$ appearing in Eq. (14) can be eliminated by using the *consistency condition*. By enforcing the slip-wear conditions, namely $F\left(\tilde{\boldsymbol{\tau}}, A\right) = 0$, $\dot{F}\left(\tilde{\boldsymbol{\tau}}, A\right) = 0$, and using Eqs. (7), (9) and (11), after performing standard steps, it follows that:

$$
\dot{\lambda} = H\left(\frac{\partial F}{\partial\boldsymbol{\tau}}\right)^T\dot{\boldsymbol{\tau}} \tag{17}
$$

where H is the *hardening* (softening) *function*, defined as follows:

$$
H := \left[\left(\frac{\partial F}{\partial A}\right)^2\left(\frac{\partial^2\psi^{in}}{\partial\alpha^2}\right) - \left(\frac{\partial F}{\partial A}\right)\left(\frac{\partial^2\psi^{in}}{\partial\alpha\partial w}\right)\left(\frac{\partial\varphi_W}{\partial W}\right) - \left(\frac{\partial F}{\partial w}\right)\left(\frac{\partial\varphi_W}{\partial W}\right)\right]^{-1} \tag{18}
$$

By summarizing, once a time-history of the total displacements $\mathbf{u}\,(t)$ has been assigned in an isothermal process, the constitutive model of the interface is defined by the state Eq. (9_1) and the three flow laws Eq. (14), containing the four unknowns $\boldsymbol{\tau}$, $\mathbf{g}$, α, w; the (not independent) variables A and W, appearing in the equations, are furnished by Eq. (11).

4 Constitutive models for no-wear friction

Models of no-wearable friction interfaces are first discussed (Fig. 6a). Since $\varphi_W = 0$, the dissipation potential, Eq. (16), coincides with the slip-function, which is taken as:

$$\varphi(\boldsymbol{\tau}, A) \equiv F(\boldsymbol{\tau}, A) = \|\boldsymbol{\tau}\| - A - \tau_0 \tag{19}$$

Here, τ_0 is a scalar, denoting the adherence limit when the interface is in its virgin state, while the thermodynamic force A accounts for isotropic hardening. Accordingly, the flow laws Eq. (14) simplify in the following:

$$\begin{aligned}
\dot{\mathbf{g}} &= \begin{cases} \mathbf{0} & \text{if } F(\boldsymbol{\tau}, A) < 0 \\ \mathbf{0} & \text{if } F(\boldsymbol{\tau}, A) = 0 \quad \text{and} \quad \dot{F}(\boldsymbol{\tau}, A) < 0 \\ \dot{\lambda}\frac{\boldsymbol{\tau}}{\|\boldsymbol{\tau}\|} & \text{if } F(\boldsymbol{\tau}, A) = 0 \quad \text{and} \quad \dot{F}(\boldsymbol{\tau}, A) = 0 \end{cases} \\
\dot{\alpha} &= \begin{cases} 0 & \text{if } F(\boldsymbol{\tau}, A) < 0 \\ 0 & \text{if } F(\boldsymbol{\tau}, A) = 0 \quad \text{and} \quad \dot{F}(\boldsymbol{\tau}, A) < 0 \\ \dot{\lambda} & \text{if } F(\boldsymbol{\tau}, A) = 0 \quad \text{and} \quad \dot{F}(\boldsymbol{\tau}, A) = 0 \end{cases}
\end{aligned} \tag{20}$$

Two sub-models are formulated ahead, exhibiting linear and nonlinear hardening behavior, respectively.

4.1 Linear hardening

The simplest state potential is quadratic in both the observable and internal variables. According to Eq. (7) (where $w = 0$), it reads:

$$\psi = \frac{1}{2}(\mathbf{u} - \mathbf{g})^T \mathbf{K}_a (\mathbf{u} - \mathbf{g}) + \frac{1}{2} k_s \alpha^2 \tag{21}$$

in which $\mathbf{K}_a$ is the *adherence matrix* that, for isotropic interface, reduces to $\mathbf{K}_a = k_a \mathbf{I}$, with k_a the scalar *adherence parameter* and $\mathbf{I}$ the identity matrix; k_s is the scalar *slip parameter*, which governs the velocity of the linear isotropic hardening. Equations (9_1) and (11_1) then supply linear laws:

$$\begin{aligned}
\boldsymbol{\tau} &= \mathbf{K}_a (\mathbf{u} - \mathbf{g}) \\
A &= k_s \alpha
\end{aligned} \tag{22}$$

As a drawback of this simplest model, it appears from Eq. (22_2) that A is allowed to tend to infinity with α, so that the adherence domain (quite unrealistically) grows unboundedly.

By using the potentials Eqs. (19) and (21) in Eq. (18), the hardening function reads:

$$H = \frac{1}{k_s} \tag{23}$$

so that, according to Eqs. (17) and (19):

$$\dot{\lambda} = \frac{1}{k_s} \frac{\boldsymbol{\tau}^T}{\|\boldsymbol{\tau}\|} \dot{\boldsymbol{\tau}} \tag{24}$$

to be substituted in the flow law Eq. (20).

4.2 Nonlinear hardening

To describe an exponential variation of hardening, the state potential Eq. (12) is modified in its inelastic part, as:

$$\psi = \frac{1}{2}(\mathbf{u}-\mathbf{g})^T \mathbf{K}_a (\mathbf{u}-\mathbf{g}) + A_\infty \left(\alpha + \frac{1}{a}\mathrm{e}^{-a\alpha}\right) \tag{25}$$

in which the new parameters A_∞ and a have been introduced. Consequently, Eq. (22_1) still holds, while Eq. (22_2) is substituted by the following:

$$A = A_\infty \left(1 - \mathrm{e}^{-a\alpha}\right) \tag{26}$$

From this latter, it follows that the thermodynamic force A is limited and approaches the upper bound A_∞ when $\alpha \to \infty$, while the parameter a governs the evolution rate; accordingly, $F(\boldsymbol{\tau}, A) < \tau_0 + A_\infty$. This model appears more realistic than the linear one, since hardening is now limited by an upper bound, preventing the unlimited expansion of the adherence domain. By comparing Eqs. (26) and (22_2), since $\mathrm{d}A/\mathrm{d}\alpha|_{\alpha=0} = aA_\infty$, it appears that $k_s = aA_\infty$ provides a linear extrapolation from the nonlinear model, valid for small values of α.

By using the state and dissipation potentials, Eqs. (25) and (19), the hardening function (18) now reads:

$$H = \frac{1}{a\,(A_\infty - A)} \tag{27}$$

and therefore:

$$\dot{\lambda} = \frac{1}{a\,(A_\infty - A)} \frac{\boldsymbol{\tau}^T}{\|\boldsymbol{\tau}\|} \dot{\boldsymbol{\tau}} \tag{28}$$

to be used in the flow laws Eq. (20).

5 Constitutive models for wear and friction

Models accounting for wear are now discussed (Fig. 6b, c). The dissipation potential is taken in the form of Eq. (16), with the slip-function still given by Eq. (19) (but expressed in terms of effective stress), and with a wear contribution $\varphi_W(W)$ added, taken as a power of W (in analogy to what is done in [2] to describe damage):

$$\varphi\left(\tilde{\boldsymbol{\tau}}, A, W\right) = \left\|\tilde{\boldsymbol{\tau}}\right\| - A - \tau_0 + \frac{\Omega}{\omega+1}\left(\frac{W}{\Omega}\right)^{\omega+1} \tag{29}$$

where Ω and ω are two parameters. Accordingly, the flow laws Eq. (14) read:

$$\begin{aligned}
\dot{\mathbf{g}} &= \begin{cases} \mathbf{0} & \text{if } F\left(\tilde{\boldsymbol{\tau}}, A\right) < 0 \\ \mathbf{0} & \text{if } F\left(\tilde{\boldsymbol{\tau}}, A\right) = 0 \quad \text{and} \quad \dot{F}\left(\tilde{\boldsymbol{\tau}}, A\right) < 0 \\ \dot{\lambda}\frac{\boldsymbol{\tau}}{(1-w)\|\boldsymbol{\tau}\|} & \text{if } F\left(\tilde{\boldsymbol{\tau}}, A\right) = 0 \quad \text{and} \quad \dot{F}\left(\tilde{\boldsymbol{\tau}}, A\right) = 0 \end{cases} \\
\dot{\alpha} &= \begin{cases} 0 & \text{if } F\left(\tilde{\boldsymbol{\tau}}, A\right) < 0 \\ 0 & \text{if } F\left(\tilde{\boldsymbol{\tau}}, A\right) = 0 \quad \text{and} \quad \dot{F}\left(\tilde{\boldsymbol{\tau}}, A\right) < 0 \\ \dot{\lambda} & \text{if } F\left(\tilde{\boldsymbol{\tau}}, A\right) = 0 \quad \text{and} \quad \dot{F}\left(\tilde{\boldsymbol{\tau}}, A\right) = 0 \end{cases} \\
\dot{w} &= \begin{cases} 0 & \text{if } F\left(\tilde{\boldsymbol{\tau}}, A\right) < 0 \\ 0 & \text{if } F\left(\tilde{\boldsymbol{\tau}}, A\right) = 0 \quad \text{and} \quad \dot{F}\left(\tilde{\boldsymbol{\tau}}, A\right) < 0 \\ \dot{\lambda}\left(\frac{W}{\Omega}\right)^{\omega} & \text{if } F\left(\tilde{\boldsymbol{\tau}}, A\right) = 0 \quad \text{and} \quad \dot{F}\left(\tilde{\boldsymbol{\tau}}, A\right) = 0 \end{cases}
\end{aligned} \tag{30}$$

As for no-wearable interfaces, two sub-models are formulated, exhibiting linear and nonlinear hardening, respectively.

5.1 Linear hardening

The state potential, according to Eq. (7), must account for wear both in the elastic and inelastic parts. As discussed in Sect. 2, wear reduces the stiffness of the stick-phase by the factor $(1-w)$; moreover, its acts as lubricant in the slip-phase, by reducing the hardening velocity. If this effect is also taken proportional to $(1-w)$, the whole potential results proportional, by the same factor, to the no-wear potential, namely

$$\psi = \frac{1}{2}(\mathbf{u}-\mathbf{g})^T \mathbf{K}_a (1-w)(\mathbf{u}-\mathbf{g}) + \frac{1}{2}k_s (1-w)\alpha^2 \tag{31}$$

The laws Eq. (9_1) and Eq. (11), then reads:

$$\begin{aligned} \boldsymbol{\tau} &= \mathbf{K}_a (1-w)(\mathbf{u}-\mathbf{g}) \\ A &= k_s (1-w)\alpha \\ W &= \frac{1}{2}(\mathbf{u}-\mathbf{g})^T \mathbf{K}_a (\mathbf{u}-\mathbf{g}) + \frac{1}{2}k_s \alpha^2 \end{aligned} \tag{32}$$

It should be noticed from Eq. (32_2) that, although wear limits the growth of the thermodynamic force A, this could still go to infinity, entailing the unbounded expansion of the adherence domain, as happens in the linear no-wear model.

Since $\partial F/\partial w = \|\boldsymbol{\tau}\|/(1-w)^2$, the hardening function (Eq. (18)) results to be the following:

$$H = \left[k_s (1-w) - \left(k_s \alpha + \frac{\|\boldsymbol{\tau}\|}{(1-w)^2}\right)\left(\frac{W}{\Omega}\right)^{\omega}\right]^{-1} \tag{33}$$

so that:

$$\dot{\lambda} = \frac{\boldsymbol{\tau}^T}{\left[k_s (1-w) - \left(k_s \alpha + \frac{\|\boldsymbol{\tau}\|}{(1-w)^2}\right)\left(\frac{W}{\Omega}\right)^{\omega}\right](1-w)\|\boldsymbol{\tau}\|}\dot{\boldsymbol{\tau}} \tag{34}$$

to be used in the flow laws Eq. (30).

5.2 Nonlinear hardening

To bound the growing of the hardening effect, the inelastic part of the state potential must be modified, by introducing an upper bound A_∞, similarly to what done for the no-wear model. Lubrication due to wear, however, reduces this limit value and the velocity whereby it is reached. Therefore, the following state potential is adopted:

$$\psi = \frac{1}{2}(\mathbf{u}-\mathbf{g})^T \mathbf{K}_a (1-w)(\mathbf{u}-\mathbf{g}) + A_\infty (1-w)\left[\alpha + \frac{(1-w)^2}{a}\mathrm{e}^{-\frac{a}{1-w}\alpha} - \frac{3}{a}\right] \tag{35}$$

From this, Eq. (32_1) follows, together with:

$$\begin{aligned} A &= A_\infty (1-w)\left[1-(1-w)\,\mathrm{e}^{-\frac{a}{1-w}\alpha}\right] \\ W &= \frac{1}{2}(\mathbf{u}-\mathbf{g})^T \mathbf{K}_a (\mathbf{u}-\mathbf{g}) + A_\infty \left\{\alpha - \frac{3}{a} + \left[\frac{3(1-w)^2 + a\alpha(1-w)}{a}\right]\mathrm{e}^{-\frac{a}{1-w}\alpha}\right\} \end{aligned} \tag{36}$$

Since $\partial A/\partial \alpha|_{\alpha=0} = a A_\infty (1-w)$, linearization of Eq. ($36_1$) around $\alpha = 0$, still leads to $k_s = a A_\infty$, when this is compared with Eq. (32_2).

By using the state and dissipation potentials, Eq. (35) and Eq. (29), the hardening function Eq. (18) reads:

$$H = \left\{a\left(A_\infty - \frac{A}{1-w}\right) - \left[A_\infty - 2A_\infty \mathrm{e}^{-\frac{a}{1-w}\alpha}\left(1-w+\frac{a\alpha}{2}\right) + \frac{\|\boldsymbol{\tau}\|}{(1-w)^2}\right]\left(\frac{W}{\Omega}\right)^{\omega}\right\}^{-1} \tag{37}$$

while:

$$\dot{\lambda} = \frac{\boldsymbol{\tau}^T}{\left\{a\left(A_\infty - \frac{A}{1-w}\right) - \left[A_\infty - 2A_\infty \mathrm{e}^{-\frac{a}{1-w}\alpha}\left(1 - w + \frac{a\alpha}{2}\right) + \frac{\|\boldsymbol{\tau}\|}{(1-w)^2}\right]\left(\frac{W}{\Omega}\right)^\omega\right\}(1-w)\,\|\boldsymbol{\tau}\|}\dot{\boldsymbol{\tau}} \tag{38}$$

must be used in Eq. (30).

6 Numerical results

Simulations, obtained via numerical integrations, are carried out for the four interface constitutive models formulated above. Results concern a rigid body sliding on a rigid surface along a rectilinear trajectory, so that the two-dimensional vector fields $\mathbf{u}(x, y)$, $\mathbf{g}(x, y)$ and $\boldsymbol{\tau}(x, y)$ reduce to scalar quantities u, g, and τ, respectively. However, also in this simplified situation, hardening and softening effects are both present and relevant.

6.1 Calibration of constitutive model parameters

In order to set-up the model parameters, the experimental results reported in [19], relevant to a monotonic history of displacements, are considered again (Fig. 2). It should be remarked that a more accurate calibration and validation of all constitutive models presented in this paper should be carried out also by using experimental results relevant to cyclic histories of displacements which, to the authors' knowledge, are not available in literature.

The parameters of the two wear models (with linear and nonlinear hardening, respectively) formulated in this paper are accordingly calibrated, in order to qualitatively and quantitatively reproduce the experimental response. However, since the linear model entails a more fast growth of stress with respect to the nonlinear model, the former must be taken much more prone to wear than the latter, in order they give comparable results, at least in a range of displacements. Results are shown in Fig. 7, where the response of a Nonlinear Hardening and Weak Wear model (NLH&WW, black curves) and that of a Linear Hardening and Strong Wear model (LH&SW, gray curves) have been plotted for two different contact pressures, namely P_1 and $P_2 > P_1$ and together with the experimental results (EXP, dashed curves). This latter effect has been simulated by modifying the interface parameter τ_0, which is indeed proportional to the contact pressure P. Moreover, the hardening parameters have been chosen in order that both models describe the same tangent in the first slip-phase. The stick-slip transition points of the curves have been marked with black dots.

The numerical values assumed by the parameters are the following. (a) For both models, $k_a = 30{,}000\,\mathrm{kN/m^3}$, $\tau_0 = 50\ \mathrm{kN/m^2}$ when $P = P_1$, and $k_a = 50{,}000\ \mathrm{kN/m^3}$, $\tau_0 = 80\ \mathrm{kN/m^2}$ when $P = P_2$; moreover, $\omega = 0.7$ for both loads; (b) for LH&SW: $k_s = 20{,}000\ \mathrm{kN/m^3}$, $\Omega = 0.0013\ \mathrm{kN}$ when $P = P_1$, and

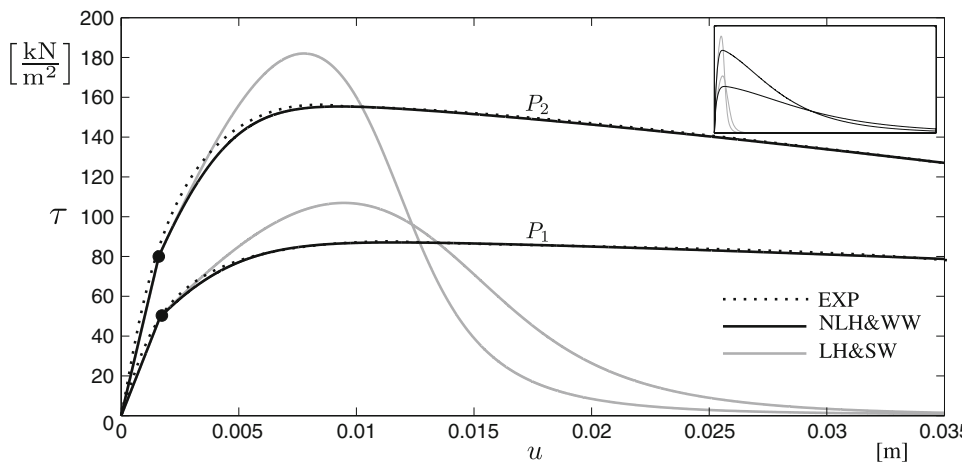

Fig. 7 Wear model responses for a monotonic displacement-history; *box*: responses for larger displacements

Table 1 Parameters for numerical simulations

	k_a (kN/m^3)	τ_0 (kN/m^2)	k_s (kN/m^3)	A_∞ (kN/m^2)	a (m^{-1})	Ω (kN)	ω
LH	50,000	80	56,000	–	–	–	–
NLH	50,000	80	–	80	700	–	–
LH&SW	50,000	80	56,000	–	–	0.001	0.7
NLH&WW	50,000	80	–	80	700	0.15	0.7

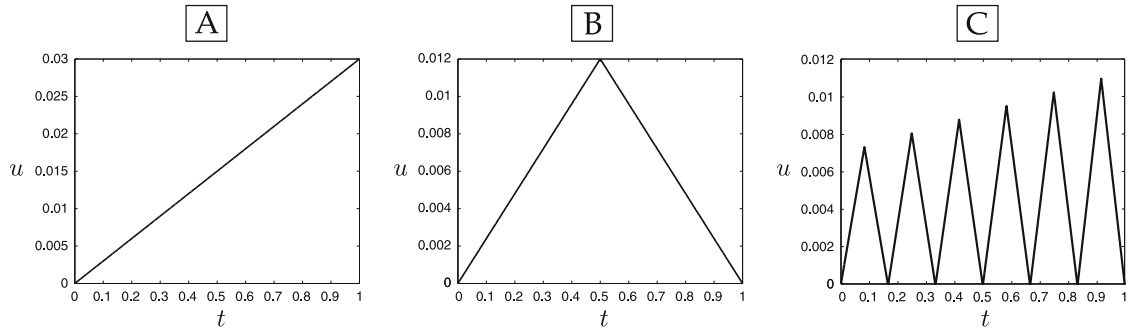

Fig. 8 Displacement time-histories

$k_s = 56{,}000$ kN/m^3, $\Omega = 0.001$ kN when $P = P_2$; (c) for NL&WW: $A_\infty = 40$ kN/m^2, $a = 500$ m^{-1}, $\Omega = 0.18$, when $P = P_1$, and $A_\infty = 80$ kN/m^2, $a = 700$ m^{-1}, $\Omega = 0.15$, when $P = P_2$.

NLH&WW model reproduces in a very accurate way the experimental results of Fig. 2, while the LH&SW model, due to its strong softening, gives a good prediction only close to the starting of the slip-phase. When the phenomenon is observed on a larger range (see the box in Fig. 7), the NLH&WW model behaves as the linear one, since the stress goes to zero when the displacement tends to infinity. This phenomenon represents the tendency to the complete smoothing of the interface, whose occurrence is faster when the contact pressure is higher.

The numerical analysis carried out ahead refers to a selected contact pressure, taken equal to P_2. To permit a direct comparison, the same parameters chosen for the wear models are used for no-wearable models, namely linear hardening (LH) and nonlinear hardening (NLH). All the numerical values are summarized in Table 1. The four models were subject to the same displacement time-histories, as plotted in Fig. 8, namely (A) a large-amplitude monotonic, (B) a medium-amplitude forward-backward and (C) a medium-amplitude cyclic. Responses were evaluated in terms of stress, gap and, if any, wear evolutions, as discussed in the following sub-sections.

6.2 Linear hardening and nonlinear hardening no-wearable models

The response of the LH interface to the three displacement histories of Fig. 8 is illustrated in Fig. 9, as stress-displacement (first column) and gap-time (second column) plots. In the monotonic history (Fig. 9a, b), the stick-phase (no gap) and slip-phase (linearly increasing gap) appear; however, stress and isotropic hardening increase unboundedly in an unrealistic way. In the forward-backward history (Fig. 9c, d), a third phase adds itself, during which the total displacement decreases. This entails an elastic unload of the interface (i.e. no gap), since the slip-threshold strongly increased in modulus during the forward phase. In the cyclic history (Fig. 9e, f), the slip-threshold progressively increases; unloading are all elastic, so that the slip-phases all occur in the positive direction, this entailing the gap always increases.

The NLH model is now considered, whose results are displayed in Fig. 10. When the model is subjected to monotonic history (Fig. 10a, b), a strongly nonlinear evolution of the stress and a weakly evolution of the gap are observed in the slip-phase. In particular, hardening reaches saturation, so that the stress cannot overcome an upper bound $\tau_{\max}$, while the gap increases. When a forward-backward history is applied (Fig. 10c, d), an elastic unloading occurs, followed by a slip-phase in negative direction, during which the stress remain constant at the saturation value $-\tau_{\max}$, while the gap experiences a weakly nonlinear decreasing. It is worth noticing that, whereas the total displacement $u = 0$ at the end of the process, a residual gap g does exist (this entailing an elastic displacement of the asperities $u^e = -g$, see Fig. 4a). When a cyclic history is considered

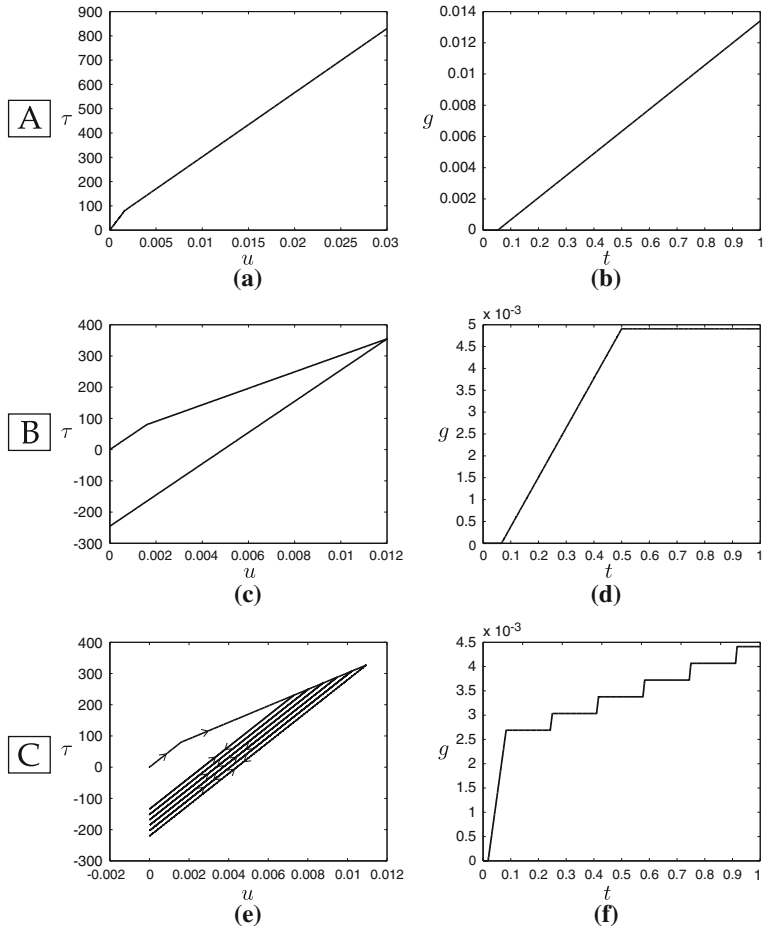

Fig. 9 LH interface response

(Fig. 10e, f), the slip-threshold stabilizes when the hardening saturates; moreover, the elastic unloading are always followed by backward slips. Accordingly, the gap evolves with increments of increasing modulus and opposite in sign during the forward/backward slip-phases.

6.3 Linear hardening and nonlinear hardening wearable models

When the LH&SW model is used (Fig. 11), the response is described as stress-displacement (first column), gap-time (second column) and wear-time (third column). During the monotonic history (Fig. 11a–c), the stress (Fig. 11a) reaches a pick value; then, it decreases and tends to zero, due to the softening effect of the wear. Meantime, both the gap (Fig. 11b) and the wear (Fig. 11c) nonlinearly increase in the slip-phase, the latter tending to the limit 1 value. When the forward-backward history is applied (Fig. 11d–f), the stress (Fig. 11d) experiences an elastic unloading whose slope, however, is less than that relevant to the stick-phase. After that, a negative slip is triggered, which is soon of soft type, due to wear accumulated in the previous slip-phase. Concerning gap (Fig. 11e), this evolves during the two slip-phases in opposite directions; a residual gap persists at the end of the process. Wear (Fig. 11f) also evolves only during the slip, but, of course, it always increases. When a cyclic displacement history is imposed (Fig. 11g–i), cycles of stress are observed (Fig. 11g), with progressive decreasing values of both the slip-threshold and the slopes of the elastic unloading. The last two cycles exhibit also negative slip. Accordingly, the gap (Fig. 11h) step-wise increases in the first cycles, then decreases up to a residual value. Wear (Fig. 11i) always increases during slip.

The NLH&WW model is finally analyzed in Fig. 12. As a general result, due to its lower sensitivity to wear (see the levels of damage reached in all the simulations), a less pronounced softening manifests itself, if compared with the linear model of Fig. 11. In detail, in the monotonic history (Fig. 12a–c), a moderate softening

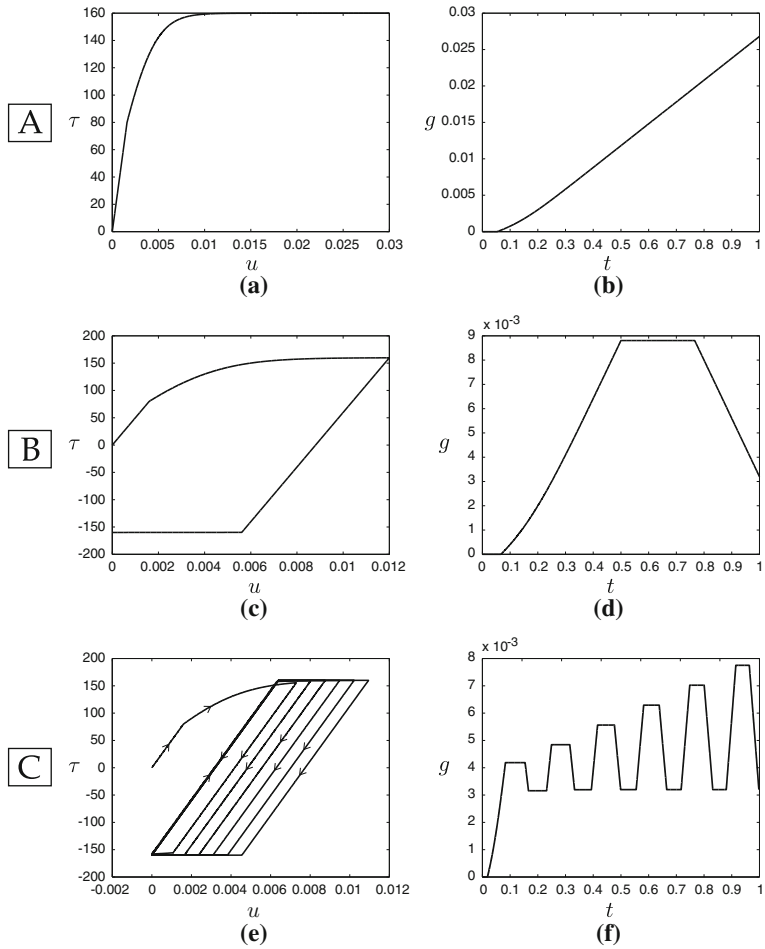

Fig. 10 NLH interface response

is observed in the evolution of stress (Fig. 12a), accompanied by values of gap (Fig. 12b) comparable with those in Fig. 11b, but much lower wear (Fig. 12c). In the forward-backward history (Fig. 12d–f), the stress (Fig. 12d) experiences an elastic unloading occurring at a slope only slightly lesser than the initial one; moreover, the negative sliding is of soft type because of the accumulated wear and due to the fact the hardening saturates; gap (Fig. 12e) and wear (Fig. 12f) evolve in the usual way. In the cyclic history (Fig. 12g–i), thresholds and slopes of the stress evolution (Fig. 12g) progressively reduce, and slips invert the sign at each unloading. Therefore, gap (Fig. 12h) stepwise oscillates with increasing amplitudes, while wear (Fig. 12i) stepwise increases up to moderate values.

7 Conclusions and perspectives

In this paper, a constitutive model for the planar interface of a soft body sliding on a hard body has been formulated. Model accounts for stick-slip phenomena (which is caused by friction) and for wear (which is caused by abrasion). First, a mechanical interpretation of some experimental results appeared in the literature has been tempted, based on a qualitative micro-mechanical model. This has highlighted the (well known) analogies between friction and plasticity and the (less known) analogies between wear and damage. In particular, an effect of lubrication of this latter, already known in Tribology, has been considered as the cause of softening of the interface, both in the stick- and in the slip-phases. Model has been formulated in the framework of Damage Mechanics, by introducing gap, isotropic hardening and wear as internal variables. A suitable choice of the state potential and the dissipation potential, as suggested by experimental observations, sided by a control

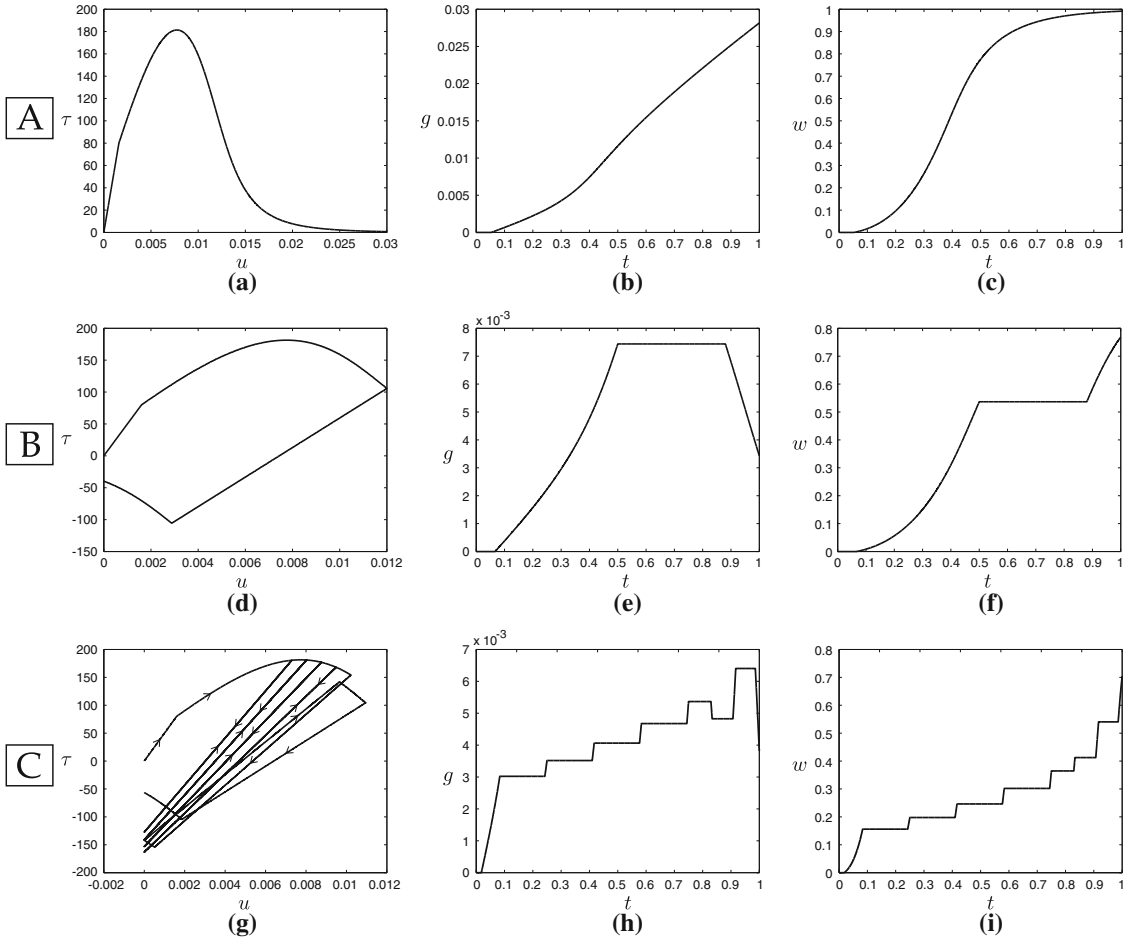

Fig. 11 LH&SW interface response

slip-function, led to state equations and flow laws for the internal variables, resulting either of associate or non-associate type.

Four different sub-models have been formulated, no-wearable or wearable, both with linear or nonlinear isotropic hardening. The parameters of the richer model have been calibrated in order to reproduce in a satisfactory way the experimental results. Then, parameters for simpler models have consistently been taken.

Simulations have been performed by numerical integrations, concerning a one-dimensional problem, in which the body moves along a rectilinear trajectory. The four models have been subjected to the same three displacement histories and results compared. The following main conclusions have been drawn.

1. The no-wearable linear hardening model leads to unrealistically high tangential stress, due to the unbounded growth of the isotropic hardening.
2. The no-wearable nonlinear model, in which hardening is limited by an upper bound, predicts a tangential stress which asymptotically tends to an upper value. Wearable models, accordingly to experimental results, are able to describe the tendency of smoothing of the considered interface. With respect to the no-wearable ones, wear induces softening, capturing the same physical phenomena and, in particular: (a) it reduces the number of the asperities at the contact interface and, as a consequence, the slope of the stick-phase decreases; (b) it reduces the resistance to the motion also in the slip phase because of the lubrication effect played by the interposed particles.
3. The strongly wearable linear hardening model is able to describe the softening behavior which follows the peak stress, as it occurs in the experimental results, as well as the degradation of the elastic properties. However, damage evolves too fast, entailing an overestimation of the lubrication (due to the quick smoothening of the interface), which fast leads the tangential stress to tend to zero in monotonic displacement

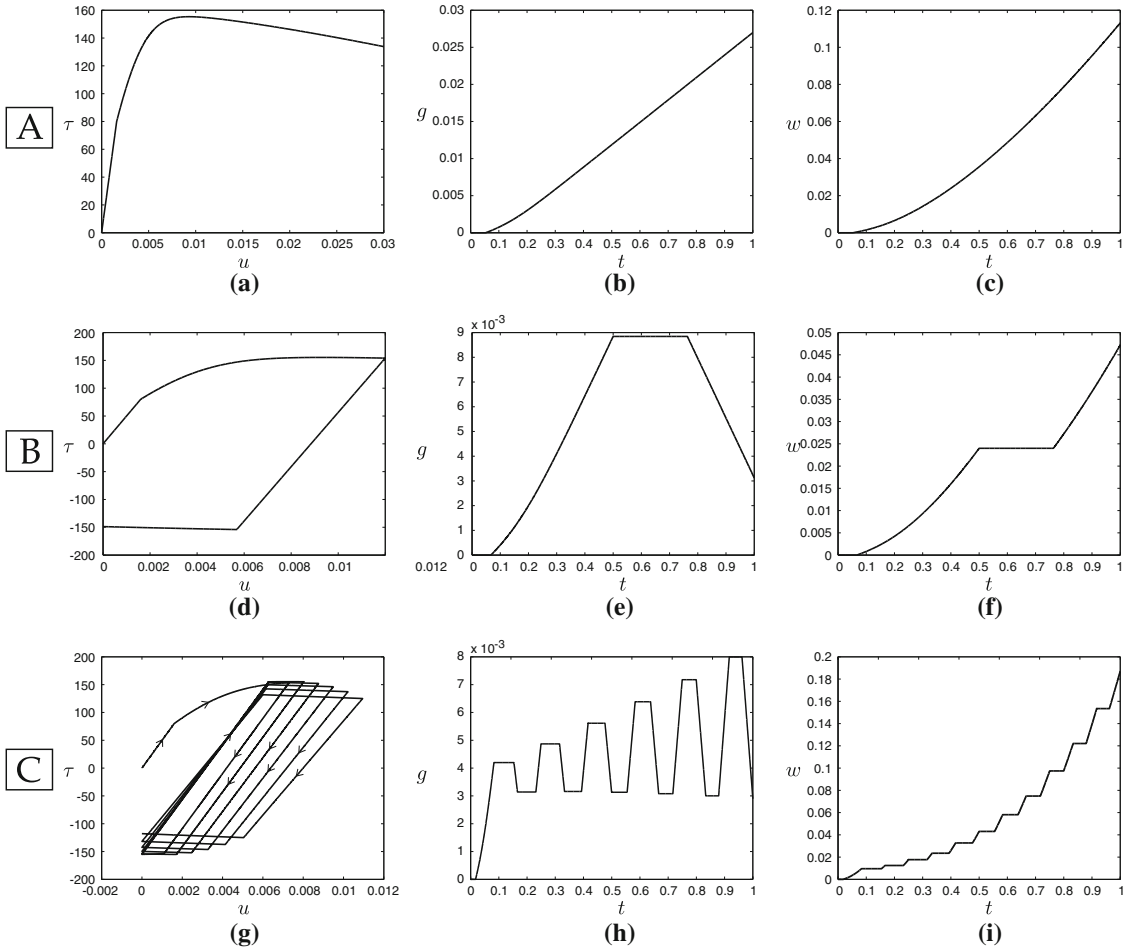

Fig. 12 NLH&WW interface response

histories, and to reduce the elastic stiffness in cyclic histories. On the other hand, a calibration of the coefficients rendering the interface less prone to wear would lead to much pronounced peaks of stress.

4. The weakly wearable nonlinear hardening model, in contrast, due to the richness of the parameters with respect to the other models, better captures the phenomenon, describing a slower damage of the interface and fitting very well the experimental results in the range in which they are available. When the numerical simulation is carried out to larger displacements, then a quite realistic tendency to the complete smoothing of the interface is observed, which entails complete lubrication and zero tangential stress.
5. Gap remains steady during the stick-phases, while it evolves, generally in a weakly nonlinear way, during the slip-phases. Increments of gap can assume both signs, according to forward-backward slips. Usually, a residual gap exists at the end of a cyclic displacement history, although the total displacement is zero. In this occurrence, gap is equal and opposite in sign to the elastic displacement of the asperities of the interface.
6. Wear also evolves only in the slip-phases, generally with a more strong nonlinear law. However, differently from gap, its increments are always positive.

As further developments, hysteretic effects, which actually are not accounted in the interface constitutive models, should be included, for example, by adapting the results presented in [51]. Moreover, constitutive equations which are used in the present paper, account for plasticity and hardening phenomena and they have to respect the physical admissibility requirements, as considered in [52]; however, an interfacial mathematical theory of the kind studied in [53,54] needs to be developed.

Analogy between friction and plasticity is stressed in this paper, even if friction is considered rate-independent, different from what is done, for example, in [55,56]; as a consequence, the interface constitutive model is analogous to one that can be defined for a ductile and damageable material. Moreover, attention is here focused

on plastic strains and damage accumulation and it could be interesting, as an improvement of the models, to account for the delamination of material layers adjacent to worn surfaces (e.g., using the method presented in [57]). This would imply, in the description of abrasive wear and damage, the introduction of model of the interface as a thick region (with non-vanishing volume) endowed with micro-structures properties, as done, for example, in [39,40,58–60]. Of course, in cited models, the structure of the continua constituting thick interfaces must be richer than that of Cauchy continua; in particular, when considering second gradient materials, the state of stress needs to be described by a second-order Cauchy stress and by a third-order hyperstress (see, e.g., [61,62]).

Finally, further work has to be done to validate the model, mainly in comparison with cyclic experimental tests, and bi-dimensional displacement histories, which are left for future investigations.

Acknowledgments This work was supported by the Italian Ministry of University (MIUR) through the PRIN cofinanced program n. 2010MBJK5B.

References

1. Lemaitre, J., Chaboche, J.L.: Mechanics of Solid Materials. Cambridge University Press, Cambridge (1994)
2. Lemaitre, J.: A Course on Damage Mechanics. Springer, Berlin (1996)
3. Lemaitre, J., Desmorat, R.: Engineering Damage Mechanics. Springer, Berlin (2005)
4. Burwell, J.T.: Survey of possible wear mechanism. Wear **1**, 119–141 (1957)
5. Stachowiak, G.W., Batchelor, A.W.: Engineering Tribology. Elsevier Butterworth-Heinemann, Burlington (2005)
6. Williams, J.A.: Wear and wear particles—some fundamentals. Tribol. Int. **38**(10), 863–870 (2005)
7. Archard, J.F.: Contact and rubbing of flat surfaces. J. Appl. Phys. **24**, 981–988 (1953)
8. Persson, B.N.J.: Sliding Friction: Physical Principles and Applications. Springer, Berlin (2010)
9. Popov, V.L.: Contact Mechanics and Friction. Springer, Berlin (2010)
10. Rabinowicz, E.: Friction and Wear of Materials. Wiley, New York (1995)
11. Maeda, K., Bismarck, A., Briscoe, B.J.: Mechanisms of scratching frictions and damage maps for rubber compounds. Wear **259**(1–6), 651–660 (2005)
12. Grosch, K.A.: Abrasion of rubber and its relation to tire wear. Rubber Chem. Technol. **65**(1), 78–106 (1992)
13. Bowden, F.P., Tabor, D.: The Friction and Lubrication of Solids, vol. I. Clarendon Press, Oxford (1950)
14. Bowden, F.P., Tabor, D.: The Friction and Lubrication of Solids, vol. II. Clarendon Press, Oxford (1964)
15. American Society of Mechanics: ASM Handbook vol. 18. Friction, Lubrication and Wear Technology. ASM International, Ohio-Usa (1992)
16. Hockenhull, B.S., Kopalinsky, E.M., Oxley, P.L.B.: An investigation of the role of low-cycle fatigue in producing surface damage in sliding metallic friction. Wear **148**(1), 135–146 (1991)
17. Kopalinsky, E.M., Oxley, P.L.B.: Investigation of the deformation and damage sustained by a wearing surface in sliding metallic friction. J. Tribol. T. Asme **117**(2), 315–320 (1995)
18. Shillor, M., Sofonea, M., Telega, J.J.: Models and Analysis of Quasistatic Contact, vol. 655, Lecture Notes in Physics. Springer, Berlin (2004)
19. Zavarise, G., Wriggers, P., Nackenhorst, U.: A Guide for Engineers to Computational Contact Mechanics. TCN, Trento (2006)
20. Mròz, Z., Stupkiewicz, S.: An anisotropic friction and wear model. Int. J. Solids Struct. **31**, 1113–1131 (1994)
21. Hjiaj, M., Feng, Z.Q., de Saxcé, G., Mròz, Z.: On the modelling of complex anisotropic frictional contact laws. Int. J. Eng. Sci. **42**, 1013–1034 (2004)
22. Malte, A.P., Böhm, M.: Different choices of scaling in homogenization of diffusion and interfacial exchange in a porous medium. Math. Methods Appl. Sci. **42**, 1257–1282 (2008)
23. Amar, M., Andreucci, D., Bisegna, P., Gianni, R.: Evolution and memory effects in the homogenization limit for electrical conduction in biological tissues. Math. Model. Meth. Appl. S. **14**(9), 1261–1295 (2004)
24. Amar, M., Andreucci, D., Bisegna, P., Gianni, R.: On a hierarchy of models for electrical conduction in biological tissues. Math. Method. Appl. Sci. **29**, 767–787 (2006)
25. Amar, M., Andreucci, D., Bisegna, P., Gianni, R.: Homogenization limit and asymptotic decay for electrical conduction in biological tissues in the high radiofrequency range. Commun. Pure Appl. Anal. **5**(9), 1131–1160 (2010)
26. Bouchitté, G., Bellieud, M.: Homogenization of a soft elastic material reinforced by fibers. Asymptot. Anal. **32**, 153–183 (2002)
27. Zmitrowicz, A.: A thermodynamical model of contact, friction and wear: 1 Governing equations. Wear **114**(2), 135–168 (1987)
28. Zmitrowicz, A.: A thermodynamical model of contact, friction and wear. 2. Constitutive-equations for materials and linearized theories. Wear **114**(2), 169–197 (1987)
29. Zmitrowicz, A.: A thermodynamical model of contact, friction and wear. 3. Constitutive-equations for friction, wear and frictional heat. Wear **114**(2), 199–221 (1987)
30. Kolmogorov, V.: Friction and wear model for a heavily loaded sliding pair 1. Metal damage and fracture model. Wear **194**(1–2), 71–79 (1996)
31. dell'Isola, F., Romano, A.: On a general balance law for continua with an interface. Ricerche Matematica **35**, 325–337 (1986)
32. dell'Isola, F., Romano, A.: On the derivation of thermomechanical balance equations for continuous systems with a nonmaterial interface. Int. J. Eng. Sci. **25**, 1459–1468 (1987)

33. dell'Isola, F., Romano, A.: A phenomenological approach to phase transition in classical field theory. Int. J. Eng. Sci. **25**, 1469–1475 (1987)
34. dell'Isola, F., Kosinski, W.: Deduction of thermodynamic balance laws for bidimensional nonmaterial directed continua modelling interphase layers. Arch. Mech. **45**, 333–359 (1993)
35. dell'Isola, F., Kosinski, W: The interface between phases as a layer, Part II. A H-order model for two dimensional nonmaterial continua. In: Rionero, S. (ed.) Waves and Stability in Continuous Media-5th International Meeting on Waves and Stability in Continuous Media vol. 4, pp. 108–113 (1991)
36. dell'Isola, F., Madeo, A., Seppecher, P.: Boundary conditions at fluid-permeable interfaces in porous media: a variational approach. Int. J. Solids Struct. **46**(17), 3150–3164 (2009)
37. Stromberg, N., Johansson, L., Klarbring, A.: Derivation and analysis of a generalized standard model for contact, friction and wear. Int. J. Solids Struct. **33**(13), 1817–1836 (1995)
38. Ireman, P., Klarbring, A., Stromberg, N.: A model of damage coupled to wear. Int. J. Solids Struct. **40**, 2957–2974 (2003)
39. dell'Isola, F., Hutter, K.What are the dominant thermomechanical processes in the basal sediment layer of large ice sheets? : Proc. R. Soc. Lond. A Mat. **454**, 1169–1195 (1998)
40. dell'Isola, F., Hutter, K.: A qualitative analysis of the dynamics of a sheared and pressurized layer of saturated soil. Proc. R. Soc. Lond. A Mat. **454**, 3105–3120 (1998)
41. Del Piero, G., Raous, M.: A unified model for adhesive interfaces with damage, viscosity, and friction. Eur. J. Mech. A Solid **29**(4), 496–507 (2010)
42. Maurini, C., Pouget, J., dell'Isola, F.: Extension of the Euler-Bernoulli model of piezoelectric laminates to include 3D effects via a mixed approach. Comput. Struct. **84**, 1438–1458 (2006)
43. Moreau, J.J.: On unilateral constraints, friction and plasticity. In: Capriz, G., Stampacchia, G (eds.) New Variational Techniques in Mathematical Physics, pp. 171–322. Edizioni Cremonese, Roma (1974)
44. Halphen, B., Nguyen, Q.S.: Sur les matériaux standard généralisés. J. Mécanique **14**, 39–63 (1975)
45. Rice, J.: Inelastic constitutive relations for solids: an internal-variable theory and its applications to metal plasticity. J. Mech. Phys. Solids **19**, 203–240 (1971)
46. Ziegler, H., Wehrli, C.: The derivation of constitutive relations from the free energy and the dissipation function. Adv. Appl. Mech. **25**, 183–237 (1987)
47. Moreau, J.J.: Application of Convex Analysis to the Treatment of Elastoplastic Systems. Lecture Notes in Mathematics, Springer, New York (1975)
48. Moreau, J.J.: La notion de sur-potential et les liaisons en élastostatique. Comptes Rendus de l'Académie Des Sciences **267**, 954–957 (1968)
49. Moreau, J.J.: Sur les lois de frottement, de plasticité et de viscosité. Comptes Rendus de l'Académie Des Sciences **271**, 608–611 (1970)
50. Quiligotti, S., Maugin, G., dell'Isola, F.: An Eshelbian approach to the nonlinear mechanics of constrained solid-fluid mixtures. Acta Mech. **160**, 45–60 (2003)
51. Choksi, R., Del Piero, G., Fonseca, I., et al.: Structured deformations as energy minimizers in models of fracture and hysteresis. Math. Mech. Solids **4**(3), 321–356 (1999)
52. Del Piero, G.: Well posedness of constitutive equations of the kinematical hardening type. In: The constitutive law in thermoplasticity, pp. 353–377, CISM Courses and Lectures, 281. Springer, Vienna (1984)
53. Del Piero, G.: On a mathematical theory of elastic-plastic materials. Arch. Mech. **27**(2), 253–271 (1975)
54. Del Piero, G.: On the elastic-plastic material element. Arch. Ration. Mech. Anal. **59**(2), 111–129 (1975)
55. Lyakhovsky, V., Ben-Zion, Y., Agnon, A.: A viscoelastic damage rheology and rate- and state-dependent friction. Geophys. J. Int. **161**(1), 179–190 (2005)
56. Gambarotta, L.: Friction-damage coupled model for brittle materials. Eng. Fract. Mech. **71**, 829–836 (2004)
57. Alpas, A.T., Hu, H., Zhang, J.: Plastic-deformation and damage accumulation below the worn surfaces. Wear **162**, 188–195 (1993)
58. dell'Isola, F., Woźniak, C.: On phase transition layers in certain micro-damaged two-phase solids. Int. J. Fract. **83**, 175–189 (1997)
59. dell'Isola, F., Hutter, K.: Continuum mechanical modelling of the dissipative processes in the sediment-water layer below glaciers. Comptes Rendus de l'Academie de Sciences **325**, 449–456 (1997)
60. dell'Isola, F., Guarascio, M., Hutter, K.: A variational approach for the deformation of a saturated porous solid. A second-gradient theory extending Terzaghi's effective stress principle. Arch. Appl. Mech. **70**, 323–337 (2000)
61. Sciarra, G., dell'Isola, F., Hutter, K.: A solid-fluid mixture model allowing for solid dilatation under external pressure. Continuum Mech. Therm. **13**, 287–306 (2001)
62. dell'Isola, F., Seppecher, P.: The relationship between edge contact forces, double forces and interstitial working allowed by the principle of virtual power. Comptes Rendus de l'Academie de Sciences **321**, 303–308 (1995)